Journal of Materials Science: Materials in Medicine (2019) 30:135
https://doi.org/10.1007/s10856-019-6342-7

SPECIAL ISSUE: CESB 2019

Original Research

Stretchable collagen-coated polyurethane-urea hydrogel seeded with bladder smooth muscle cells for urethral defect repair in a rabbit model

Chengyuan Wang[1] · Chunyang Chen[1] · Mingyu Guo[2] · Bin Li[2] · Fengxuan Han[2] · Weiguo Chen[1]

Received: 9 July 2019 / Accepted: 16 November 2019 / Published online: 4 December 2019

Abstract

The major challenge to treat the clinical adverse effects of long-segment urethra is in achieving viable tissue substitution. The substituted construct's properties-such as its resilience, contraction, and ability to minimize scar-stenosis formation should be considered. In the present work, a unique polyurethane-urea (PUU) fibrous membrane is fabricated by electrospinning. Then PUU was coated by collagen and formed the elasticity hydrogel after immersed in collagen solution. Meanwhile, the cPUU hydrogel exhibited a fibrous microstructure. This cPUU hydrogel had outstanding stretching property with 404 ± 40% elongation at break compared with traditional hydrogels, which satisfied the requirement of urethra. The cPUU hydrogel also supported the adhesion and growth of bladder smooth-muscle cells (BSMCs) in natural state cell morphology. Urethral defects in New Zealand male rabbits were repaired with cPUU seeded with BSMCs in vivo. After three months, more smooth-surface area of reconstructed urethral tissues was observed in the cPUU hydrogel-BMSCs groups compared with that of the control group. The luminal patency and the incidence of complications-including calculus formation, urinary fistula, and urethral-stricture occurrence were significantly lower in the cPUU group compared with that of the control group. Hence, cPUU fibrous hydrogels are promising scaffolds for application in urological tissue engineering.

Graphical Abstract

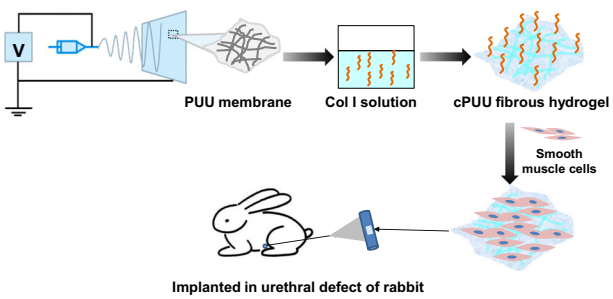

1 Introduction

Severe urethral stricture typically occurs after inflammation, malignancy, injuries, or via congenital acquisition. With a

These authors equally contributed: Chengyuan Wang, Chunyang Chen

✉ Bin Li
binli@suda.edu.cn

✉ Fengxuan Han
fxhan@suda.edu.cn

✉ Weiguo Chen
cwgms123@163.com

[1] Department of Urology, The First Affiliated Hospital, Soochow University, Suzhou, Jiangsu 215006, China

[2] Orthopaedic Institute, College of Chemistry, Chemical Engineering and Material Science, Soochow University, Suzhou, Jiangsu 215006, China

history of being a difficult problem for urologists, conventional treatments for urethral stricture have involved use of the buccal mucosa or the foreskin flap for grafts in urethral-injury therapy [1]. In addition to the trauma induced in the donated location, curling, contracture, and ectopic secretion of the graft may increase the possibility of stenosis recurrence [2]. If stenosis exists, it can cause many complications, such as erectile dysfunction, erectile pain, and increased risks of urinary fistula and lithogenesis [3, 4]. Therefore, the development of an ideal biomaterial to repair urethral defects is an ongoing clinical goal.

Emerging tissue-engineering strategies possess the prospect to fabricate biological substitutes that may assist in the anatomical and functional reconstruction of the original urethra [5, 6]. Ideal biomaterials not only require reliable biocompatibility, but must also promote cell adhesion, interconnection and production of the extracellular matrix (ECM) [7]. Additionally, the appropriate strength and flexibility of biomaterials to adapt to physiological activities are equally crucial factors for urethral repair, especially when the urethra will be needed for erections [8]. At present, materials used in urethral tissue engineering are generally classified as acellular matrices and polymers, which include both synthetic polymers and naturally derived polymers [9]. Acellular matrices derived from harvested tissues and organs exhibit the possibility to retain the majority of useful constituents of the natural ECM, while reducing any resident cellular components and exogenous immune responses. This feature promotes cellular proliferation and differentiation into similar cellular types in situ. In spite of this, the smooth surface of the acellular matrix makes it difficult for cells to accumulate to a sufficient thickness [10]. Natural polymers include collagen, fibrinogen, gelatin, alginate, and silk [11]. Among them, collagen is an important component of connective tissue that is widely used in tissue engineering and accounts for 25–30% of total mammalian proteins, and has low immunogenicity [12, 13]. In a previous study, collagen scaffolds modified with vascular endothelial growth factor were used in a canine model with extensive urethral defects [14]. However, the mechanical strength of collagen itself is very weak, and it is usually used for coating or mixing with other materials.

Synthetic polymers include polylactic acid (PLA), polylactide-*co*-caprolactone (PLCL), polylactic-*co*-glycolic acid (PLGA) and Pluronic F-127. Some of these synthetic polymers have a long history of use in tissue engineering. Scaffolds with different mechanical strengths and surface microstructures can be prepared via different methods. Two-dimensional films of PLGA and PCL, made by the spin-coating method, have confirmed their biocompatibilities for the growth of human urethral-epithelial cells and smooth-muscle cells. In the same study, the researchers found that the elastic modulus was a significance characteristic, where it was not only defined as a mechanical aid but also had a biological impact on cells and tissues [15]. Polyurethane-urea (PUU), synthesized by Guo et al., has a supramolecular structure with a longer hydrophobic-spacer force that can resist a stronger hydrogen-bonding unit (urea), which exhibits considerable elasticity, strength, and a high water-containing capacity [16]. Hence, this kind of supramolecular PUU may have potential for broad applications in urethral repair.

Hydrogels have been widely used in tissue engineered tissue due to their unique compositional and structural similarities to the natural extracellular matrix, in addition to their desirable framework for cellular proliferation and survival [17, 18]. Fiber scaffolds have also attracted attention because of their similar structure to natural extracellular matrices [19, 20]. Therefore, the hydrogel fibers combining the advantages of hydrogel and fibers may have potential application in tissue engineering. Electrospinning are considered to be suitable methods for preparing hydrogel microfibers. In our previous studies, we have prepared electrospun membranes which support cell growth. Specially, the electrospun PLA/poly(ethylene glycol) scaffolds seeded with human amniotic mesenchymal stem cells showed well repair result for urethral epithelium [21]. To further improve the surface bioactivity of scaffolds, surface coating is an effective approach [22]. In a study, Yang et al. prepared porous $Se@SiO_2$ nanosphere-coated catheter, and found that this catheter could accelerate prostatic urethra wound healing by modulating macrophage polarization through reactive oxygen species-NF-κB pathway inhibition [23]. Recently, an insulin-like growth factor 1 sustained-release collagen urethral catheter was used to repair urethral injury in a rabbit model [24]. This coating significantly improves wound healing and prevents urethral stricture after urethral injury.

In this study, we have improved the microstructure and surface composition of a novel scaffold by filling the electrospun fibers with collagen. The cPUU hydrogel was fabricated by soaking supramolecular PUU membrane in diluted collagen. The cPUU was stable in retaining the microstructure and mechanical strength. Both the surface morphology and compositional change of the cPUU were detected in this study. Furthermore, we used bladder smooth-muscle cells (BSMCS) to evaluate the cytocompatibility of the scaffold. To investigate the repairing effects of cPUU in vivo, the scaffold-seeded with BSMCs was implanted into a rabbit model of urethral defects. Three months after the operations, the urethras of these rabbits were analyzed via imaging and histological analysis.

2 Materials and methods

2.1 Materials

The hydrophobically modifed linear PUU (Mw = 380000 g/mol) copolymer synthesized a newly designed one-pot approach [16] was supported by professor Guo. Bovine type-I collagen was purchased from Thermo Fisher Scientific, USA. Fetal bovine serum (FBS), 0.25% penicillin-streptomycin, and 0.05% trypsin containing 0.53 mM ethylenediaminetetraacetic acid (EDTA) were purchased from Gibco, USA. Dulbecco's modified Eagle medium (DMEM) was supplied by Hyclone (USA). Type-I collagenase was provided by sigma, USA. A Cell Counting Kit-8 (CCK-8) was purchased from Dojindo Molecular Technologies, Inc., Japan. Alexa Fluor™ 488 Phalloidin (Invitrogen™) and (4',6-diamidino-2-phenylindole) DAPI were purchased from Thermo Fisher Scientific (China) Co., Ltd. Hexafluoroisopropanol was purchased from China Sun Specialty Products Co., Ltd., China.

2.2 Preparation of cPUU hydrogel

To obtain PUU electrospun fibrous films, electrospun solution containing 12 (wt/wt) % PUU in hexafluoroisopropanol were prepared. The solution was injected at a flow rate of 1.5 mL/h, and 12.8 kV of high voltage supplied by a high-voltage power supply (DonWen High Voltage Inc., China). There is an air gap distance of 15 cm between the needle and the grounded aluminum foil collector. The fresh fibrous membranes were peeled off from the aluminum foil and were dried in a vacuum oven at room temperature to remove the residual organic solvents. The cPUU hydrogels were prepared by immersing a piece of PUU fibrous film in 10% Bovine collagen solution at 37 °C for 24 h. Bovine collagen solution was purchased from Thermo Fisher Scientific, USA. After the film drained with a filter and sealed with plastic wrap, the cPUU hydrogel was stored at 4 °C.

2.3 Characterizations

The morphology of the scaffold was observed by using a scanning electron microscope (SEM, S-4800, Hitachi, Tokyo, Japan). Before SEM imaging, the dried scaffolds were sputtered and coated with gold using a Hummer V sputtering system (Technics Inc., Baltimore, MD, USA) at 50 mA to obtain a 10-nm coating. The average fiber diameters and scaffold thicknesses of the electrospun scaffolds were quantitatively analyzed from SEM micrographs using Image J 1.31 v software (National Institutes of Health, Bethesda, MD, USA). In order to measure the compositional difference between PUU and cPUU, the Fourier-transform infrared-spectroscopy (FTIR) spectrum was measured in the range of 400–4000 cm^{-1} using a FTIR spectrometer (NICOLET6700, Thermo Fisher Scientific Inc., USA).

2.4 Mechanical testing

All of the films were made into dumbbell-shaped strips (5 cm in length, 1 cm in width at ends of the dumbbell shape and 0.2 cm in width of center). Before testing, these films were immersed in serum-free medium for 30 min. The mechanical properties of the materials were tested by using an Instron E10000 system (INSTRON Inc. Canton, MA, USA) at a constant crosshead speed of 10 mm/min. The wall thickness of the cPUU-hydrogel membrane was measured by a digital-calibrated caliper. The young's modulus, stress at break and strain at break were determined by using the manufacturer's software.

2.5 BSMC isolation and expansion

To obtain BSMCs, one fresh bladder of a healthy New Zealand white rabbit was harvested with a sterile scalpel after being euthanized with chloral hydrate. Then, the muscular layer of bladder tissue was micro-dissected. The muscle tissues were minced and digested with 0.5 wt% type-I collagenase. After 30 min, the suspended cells were filtered through a 74-μm cell strainer and were then cultured in DMEM supplemented with 10% FBS to obtain BSMCs.

2.6 BSMC proliferation and viability

To prepare electrospun scaffolds for cell culture, the electrospun fibers were collected on circular-glass cover slips (14 mm in diameter) and were fixed on 24-well plates with polydimethylsiloxane (PDMS) rings. Before cell culture, these electrospun scaffolds were disinfected by immersing in 75% ethanol for 2 h, and were then washed three times with phosphate-buffered saline (PBS).

The proliferation and viability of BSMCs on cPUU scaffolds were evaluated using a CCK8 assay. Three groups were used in this experiment, including a blank control group, PUU group, and cPUU group. Four duplicates were tested in each group. One hundred microliter of BSMC cell suspensions (50,000 cells/mL) were seeded into the control well or scaffolds. Then, 300 μL of culture medium was supplemented and the wells were incubated at 37 °C with 5% CO_2. At 1, 3, 5, and 7 d, the culture medium was replaced with 400 μL of fresh medium containing 40 μL of CCK-8 reagent. The optical density (OD) value at 450 nm was obtained by a microtiter plate reader (BioTek, USA).

To investigate the cell morphology on the scaffold, one hundred microliter of BSMC cell suspension (50,000

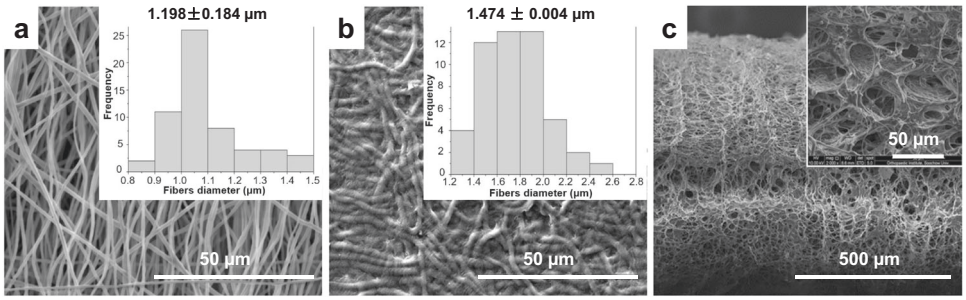

Fig. 1 SEM micrographs of PUU fibrous scaffold and fiber diameter distribution. **a** SEM micrographs of PUU fibrous scaffold; **b** SEM micrographs of cPUU scaffold; **c** section morphology of PUU fibrous scaffold by SEM

cells/mL) was seed on the surface of PUU, cPUU and tissue culture plate, respectively. All the groups were incubated for 3 days. Then all the groups were washed with PBS, and fixed with 4% paraformaldehyde. Alexa Fluor™ 488 Phalloidin was used for cytoskeleton staining, and DAPI was used for nuclear staining. The images of different group were collected by an inverted fluorescence microscope.

2.7 Animal experiments

Twenty-four male New Zealand white rabbits (three months-old, 2.5–3.0 kg) were used in the experiments. All rabbits were anaesthetized with pentobarbital and each rabbit had a 8-Fr transurethral catheter inserted in situ. Through a ventral-midline penile-skin incision, the urethra was separated from the corpora. A ventral urethral defect, with a mean length of 1.5 cm and mean width of 0.8 cm, was formed in the rabbit anterior urethra about 2 cm away from the urinary meatus. Urethral defects were sutured continuously with 6-0 vicryl sutures. The catheters were fixed with sutures on the foreskin to protect bladder function for seven days after the operation.

After operation, these rabbits were divided into three groups. In group A (the experimental group), eight animals were implanted with cPUU-fibrous hydrogels. In group B, eight rabbits were implanted with PUU scaffolds. In group C (the negative-control group), eight rabbits were sutured directly. The electrospun scaffolds were trimmed and placed over the defect as an onlay.

All animals were killed at three-months post-implantation. Before euthanasia, the urethral caliber was assessed with retrograde urethrography. The contrast agent iodofol was injected into the urethra and the urinary meatus was closed with tweezers. Subsequently, the CT images were analyzed. Urethral stricture and urinary fistula in each group were evaluated by analyzing the width of urethral imaging in the CT images and whether there was leakage of contrast agent into space in the body. The whole urethra was excised and the entire urethral mucosa was observed. Section (5-mm lengths) were fixed with formalin, and then paraffin wax-embedded tissues were cut into 0.8-mm slices and were stained with H&E. Next, a-SMA immunohistochemical staining was utilized to verify the presence of smooth-muscle cells in the repaired urethra. Image Pro Plus 5.1 software (Media Cybernetics, Inc., MD, USA) was used to quantify positive staining in 10 different areas for each tissue sample. The animal surgery protocol was approved by the Institutional Animal Care and Use Committee (IACUC) of Soochow University.

2.8 Statistical analysis

All quantitative data are presented as mean ± standard deviation, with no less than triplicates being included for each group. SPSS statistical software 16.0 (Chicago, IL, USA) was used to calculate inferential statistics by one-way analyses of variance. Unpaired Student's t tests were also used where appropriate. Difference between the groups was considered statistically significant if $p < 0.05$.

3 Results

3.1 Characterization of cPUU hydrogels

To observe changes of PUU films coated with collagen, we examined the morphologies of nanofibers and their hydrogel-binding reactions by SEM images. Different fiber-diameter distributions of PUUS and cPUU are presented in Fig. 1. During the preparation of cPUU scaffolds, there were changes in the dimensions of the PUU-fibrous scaffolds (Fig. 1a, b). The preceding fibers were loose (Fig. 1a). The average diameter of the PUU fibers was 1.198 ± 0.184 μm. After soaking in collagen, the cPUU became a transparent hydrogel and the diameter of the cPUU increased due to water absorption and swelling (Fig. 1b). The average diameter of the cPUU was 1.474 ± 0.004 μm. Moreover, there were obvious fibrous microstructures on the surface of cPUU film, which could support cell adhesion and growth. The porous structure of PUU was also easily observed in the cross section (Fig. 1c).

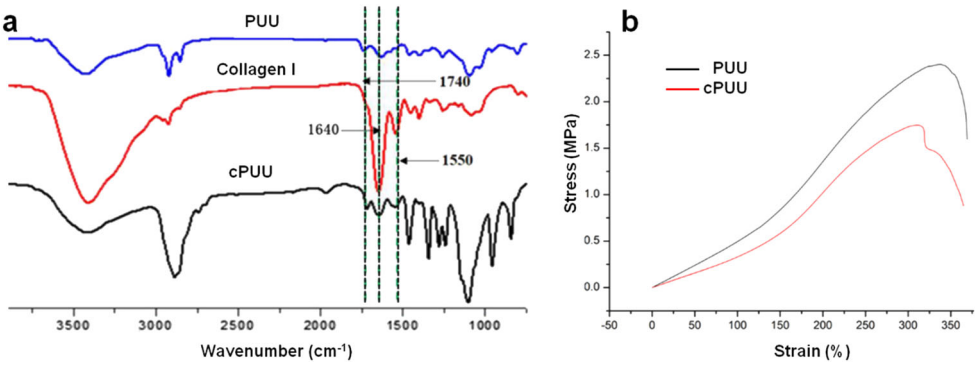

Fig. 2 **a** FTIR spectra of collagen I, PUU and cPUU scaffolds. **b** typical strain-stress curve of cPUU fibrous hydrogel

Table 1 Mechanical properties of the grafts

Sample	Peak stress (MPa)	Modulus (MPa)	Strain at break (%)
PUU	3.1 ± 0.63	7.8 ± 0.67	437 ± 59
ccPUU	1.9 ± 0.91	5.4 ± 2.0	404 ± 40

The FTIR spectra of collagen I, PUU and cPUU are shown in (Fig. 2a). The FTIR spectra displayed by PUU were similar to those reported previously [18]. For the PUU material, the peak of 1740 cm^{-1} mainly indicated the coexistence of H-bonded C=O from urethane groups and free C=O from urea groups. The peak value at 1640 cm^{-1} demonstrated pronounced urea-urea H bonding for maintaining the PUU. Among type-I collagen, there were two peaks near 1640 cm^{-1} and 1550 cm^{-1}, and the amplitude was relatively larger at 1640 cm^{-1}. These two characteristic absorption peaks mainly corresponded to amide-I bonding and amide-II bonding in collagen. After collagen coating, cPUU showed both the typical peaks of PUU and collagen. These results showed that type-I collagen was successfully modified onto the PUU scaffold. The mechanical strengths of PUU and cPUU were measured and compared with the mechanical strength of natural urethra in previous studies. The typical strain-stress curve is shown in (Fig. 2b). The PUU and cPUU had similar peak stress at beak, as shown in Table 1. However, the elongation of cPUU showed slightly reduced compared with that of the PUU (Table 1). The strain at break of cPUU was 404 ± 40%.

3.2 Cell proliferation and viability

BSMCs proliferated on both PUU and cPUU hydrogels were detected by a CCK-8 assay. (Fig. 3a). At the first day, the optical density (OD) values of the three groups were similar, indicating that both PUU and cPUU hydrogels had no significant toxicity to BSMCs. The OD values of the cPUU group at five and seven days were higher than those of the PUU group, and these differences were statistically significant. These results suggest that cPUU hydrogel is a promising biomaterial for biomedical applications.

The growths of BSMCs cultured on tissue culture plates, PUU- and cPUU-hydrogels for three days were also analyzed by skeletal staining (Fig. 3b–d). The results showed that BSMCs grew well on cPUU and PUU scaffolds. The cells on the cPUU scaffold were closer to that of natural growth than those in the blank-control group and PUU group. The morphology of BSMCs wasmore widely distributed on the cPUU hydrogels than those of the other two groups. These results demonstrated that collagen coating could promote cellular recovery when grown on PUU material.

3.3 In vivo evaluation of cPUU scaffolds

The cPUU hydrogels were used to evaluate the repair of urethral defects in rabbits (Fig. 4a). All of the rabbits survived until they were killed. Both cPUU and PUU materials were rectangular in size (1.5 × 0.8 cm). At the sixth week, the urethral defect treated by direct suturing displayed an obvious scar and fistula (Fig. 4b). Gross viewing of the reconstructed urethra with PUU also showed a scar and fistula (Fig. 4c). In the cPUU group, gross viewing showed that the material in the urethra was indistinguishable from that of the surrounding tissue, and the reconstructed surface of the urethra was smooth and a continuous mucosa could be seen at the sixth week after operation (Fig. 4d). When the observation time was extended to 12 weeks in the cPUU group, no obvious scar formation was found on the mucosa surface of the urethra, and no obvious crystallization was found in the urethra. In the PUU group, the urethral mucosa was absent, and the tendency of urinary fistula appeared at the sixth week, and after the sixth week the urinary fistula appeared with scar formation, but without obvious crystallization. In the direct-suture group, the surface of the urethral defect was uneven and there was scar formation, mucosal contraction and lumen narrowing at six weeks after operation. At 12 weeks, urethral stricture was evident and no obvious crystal-like substance was found, but the incidence of urethral fistula increased compared with that of the former two groups.

At the 12th week, three groups of animals underwent CT urethrography to quantitatively analyze the occurrence of

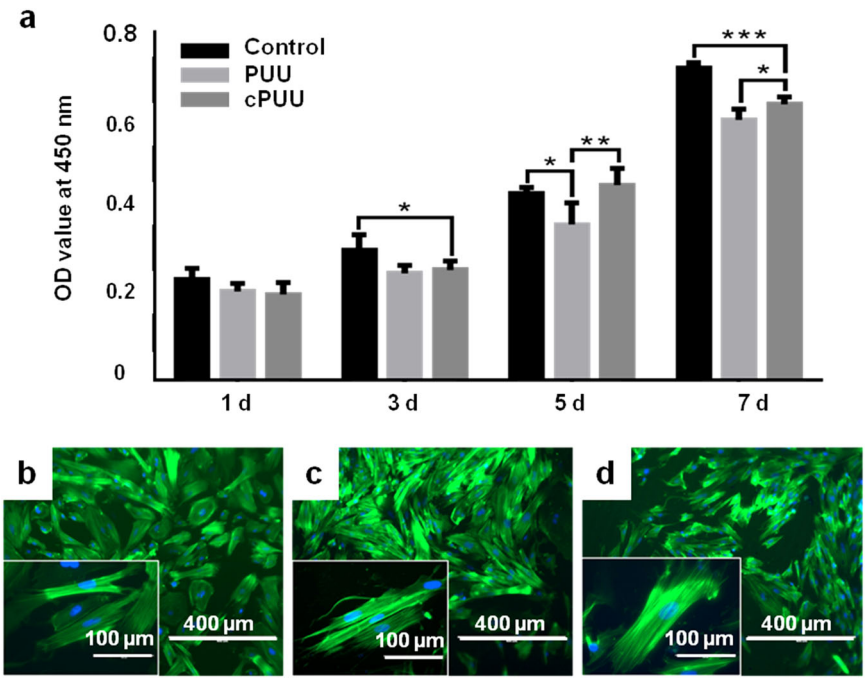

Fig. 3 **a** CCK-8 assay of BSMCs on blank control, PUU and cPUU hydrogels at 1d, 3d, 5d, 7d. $*p < 0.05$, $**p < 0.01$, $***p < 0.001$. F-actin staining of BSMCs labeled by fluorescein isothiocyanate on blank control (**b**), PUU (**c**) and cPUU (**c**)

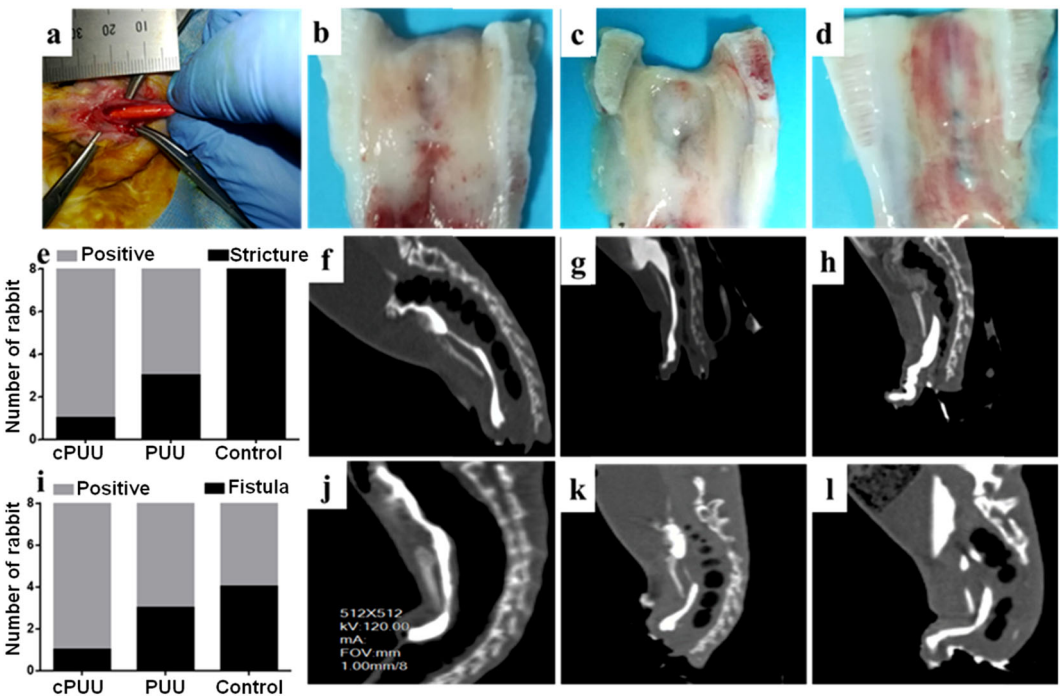

Fig. 4 **a** Creating extensive urethral defect in a New Zealand white rabbit. Representative gross photographs of reconstructed urethra of direct suture group, PUU and cPUU groups at 12 weeks (**b**–**d**). The quantitative data of stricture and fistula occurrence at 12 weeks (**e**, **i**). urethrography images of direct suture group (**f**), PUU group (**g**) and cPUU group (**h**) at 6 weeks. Urethrography images of direct suture group (**j**), PUU group (**k**) and cPUU group (**l**) at 12 weeks

urethral stricture (Fig. 4e–l). Urography in the direct-suture group showed different degrees of urethral stricture. There were three cases of urethral strictures in the PUU group, while only one case of urethral stricture was present in the cPUU group. At 12 weeks, the stenosis in the control group was aggravated in some specimens, but no significant change was found between the PUU group and the cPUU group at the sixth week after operation. In addition, half of the control group had urinary fistula, while there was no significant urinary fistula in any of the rabbits in the cPUU

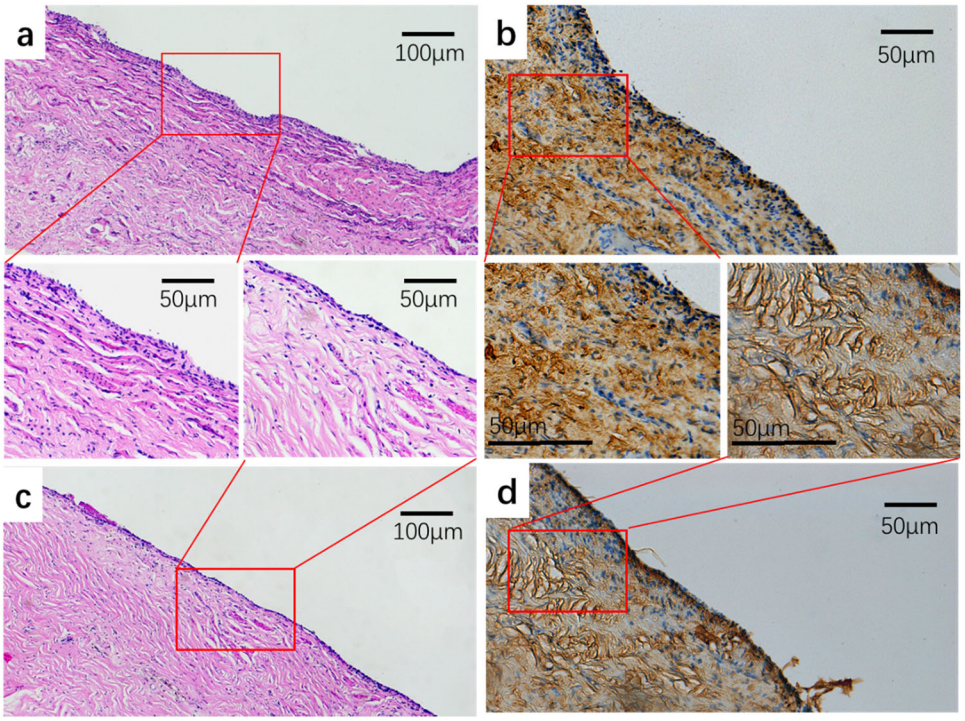

Fig. 5 Assessment of cell density in the proximal urethra of the rabbit. Representative images of cross-section of proximal urethra at 12 weeks with H&E staining of reconstructed urethra using PUU (**a**) and cPUU seeded with BSMCs (**c**). The urothelium layer of the lumen is showed at high magnification. Immunohistochemical of α-smooth actin antibody in PUU group (**b**) and cPUU group (**d**) for 12 weeks. The yellow area corresponding to smooth muscle cell density

group; there was significant difference between the two groups in terms of this parameter.

From the results of H&E staining, there was no significant difference in the content of the epithelium between the PUU group and the direct-suture group. The epithelial thickness of the cPUU group was longer than that of the other group (Fig. 5a, b). In the PUU group, a large amount of collagen accumulation was observed, which replaced the epithelium. Immunohistochemical examination of a-smooth actin antibody is shown in (Fig. 5c, d). The results showed that the smooth-muscle matrix in the cPUU group was well arranged. In addition, the muscle content of the cPUU group was higher than that of the PUU group (Fig. 5c, d).

4 Discussion

Reconstruction of large urethral defect is still a challenge in clinic. Although autologous tissues have made great progress in urethral repair, the high risk of complications such as restenosis increased with the follow-up time [25]. Regenerated urinary tract tissues should not be a role of outflow channels but also biological properties to match the physiological functions of urine stretch out and draw back [26]. Regenerative medicine and tissue engineering may provide an alternative for urethral substitutes. An ideal biomaterial is still being explored to find a urethral substitute has appropriate strength [8], rapid functional recovery and tissue regeneration rate.

To mimetic the deformation and recovery property of natural urethral tissues, the elastic material is needed. Hydrogel has good elasticity, which can recover to initial shape once the stress is removed. Moreover, hydrogel has been widely used in tissue engineering. However, the traditional hydrogels lack high stretch performance. In a previous work by Guo et al., a supramolecular PUU was synthesized and exhibited considerable elasticity, strength, and a high water-containing capacity [16]. To further enhance the cell adhesion and spread on the PUU material, replacing the smooth surface of PUU hydrogel with a rough one may be effective. Therefore, in this study, a PUU fibrous hydrogel was prepared by electrospining and subsequent hydration. There was a substantial change in dimensionality after immersion in water. After soaking in collagen, the PUU film became a transparent hydrogel and the diameter of the cPUU increased due to water absorption and swelling. However, this cPUU still exhibited fibrous structure (Fig. 1). Unlike traditional hydrogels, this cPUU fibrous hydrogel had excellent stretching property (Fig. 2). The elongation at the break was $404 \pm 40\%$ under stress of 1.9 ± 0.91 MPa, which was significantly higher than the values of natural urethra strain at break (180%) according to previous study [27]. The value of strain at break in cPUU was much higher than native urethra. In conclusion, this fibrous hydrogel will have both advantages of hydrogel and fibrous microstructure.

As a widely used material in biomedical applications, collagen forms a homogeneous and isotropic hydrogel

through hydrophobic interactions in neutral or basic solutions and a temperature of 37 °C, showing good biocompatibility and less inducing the host's immune response [28]. It has been reported that plasma and electrospinning can be used to prepare collagen nanofibers, but these processes destroyed the triple helical structure of natural collagen, as it involved the use of organic solvents with highly polar or an electric field effect [29]. Fibrous membranes made by electrospinning have macroscopic smoothness and microscale interconnected-network pores, which form the basis for supporting cell migration, nutrient penetration and blood-vessel formation [30, 31]. The coating of collagen on electrospun PUU film would further improve the bioactivity of the membrane. Furthermore, this method is simple and the production costs less. Ultimately, the fibrous microstructure and collagen on the surface of cPUU membrane, could facilitate cell adhesion and growth.

Suitable seed cells will be benefit for repairing urethral defect. In previous experiments, a variety of seed-cell scaffolds have been implanted to repair urethral defects, such as bone-marrow stem cells, urinary stem cells, adipose-derived stem cells, urethral-epithelial cells, smooth-muscle cells and other cell types [32]. These cells affect the prognosis of urethral-defect sites and the recovery of urinary function through paracrine or related mechanisms [33]. However, these seed-cell scaffolds currently cannot be used in the clinic due to ethical considerations and environmental regulations. Without reliable supportive data from translational animal models, it is still difficult to ensure the future implementation of seed-cell scaffolds in the clinic. Therefore, in this study, we choose BSMCs as seeds because of their homology and minimal risk for inducing autoimmune responses [34, 35]. Hence, BSMCs, supplemented by materials with controllable mechanical properties and surface microstructures, may be a reliable choice for translational research for improving urethral-stricture reconstruction [36]. The results showed that BSMCs can grow on the surface of cPUU (Fig. 3). Moreover, the morphology of BSMCs was more spread on the cPUU hydrogels than those of the other two groups.

The in vivo evaluation also showed that the cPUU group seed with BSMCs had better repair results. More smooth mucosa surface of the urethra in ccPUU group were found by gross viewing. Through CT-urethrography image, the cPUU seemed to reduce the complications of urinary fistula and stricture after urethral reconstruction. It also had obvious advantages in local tissue repair. Paraffin sections showed that cPUU scaffolds could promote epithelial-tissue regeneration and reduce excessive collagen accumulation. Furthermore, the cPUU also reduced the incidence of scar stenosis.

There were several limitations of the present study. Although the degradation of the PUU scaffold could disappear after three months which can infer from our results, longer-term implication to human body could still lead to foreign-body reactions and increase lithogenesis. In addition, harvesting cells from patients with urothelial carcinomas has been shown to increase the risk of tumor recurrence [37]. Moreover, Subramaniam et al has highlighted that urothelial cells derived from bladders with neuromuscular dysfunction yielded poor regenerative capability when cultured in vitro [38].

5 Conclusions

In conclusion, cPUU fibrous hydrogels were successfully prepared by coating PUU electrospun scaffolds with collagen I in this study. After immersing into water, the electrospun cPUU changed into fibrous hydrogel. The cPUU hydrogel showed a fibrous microstructure of the electrospun fibers, although the fiber diameter increased by 70% compared with that of the PUU electrospun fibers. The stretchable hydrogels of cPUU exhibited considerable stretching properties with 404 ± 40% elongation at break, which was higher than natural urethral tissue. Moreover, the cPUU could support BSMCs to adhere and proliferate in vitro. According to the results from urethral morphology, tissue reconstruction, luminal patency, and complication incidence (including stone formation, urinary fistula, and urethral stricture) among the animals, the cPUU hydrogels could be used for repairing urinary-tract defects. Furthermore, histological evaluations showed that the cPUU hydrogels, seeded with BSMCs, promoted the re-epithelialization of local urethral defects. Taken together, these results indicate that the cPUU has potential application in urinary-tract tissue engineering.

Acknowledgements This study was supported by the National Key R&D Program of China (2016YFC1100203), National Natural Science Foundation of China (81672213, 31872748), Jiangsu Provincial Clinical Orthopedic Center, and the Priority Academic Program Development (PAPD) of Jiangsu Higher Education Institutions.

Authors' contributions Weiguo Chen, Fengxuan Han and Bin Li conceived and designed the experiments; Professor Mingyu Guo provided the PUU materials; Chunyang Chen and Chengyuan Wang performed the experiments with the help of Fengxuan Han; Chunyang Chen and Chengyuan Wang analyzed the data; Chengyuan Wang and Fengxuan Han wrote the paper.

Compliance with ethical standards

Conflict of interest The authors declare that they have no conflict of interest.

References

1. Xu YM, Qiao Y, Sa YL, Zhang J, Fu Q, Song LJ. Urethral reconstruction using colonic mucosa graft for complex strictures. J Urol. 2009;182:1040–3.
2. Barbagli G, Kulkarni SB, Fossati N, Larcher A, Sansalone S, Guazzoni G, et al. Long-term followup and deterioration rate of anterior substitution urethroplasty. J Urol. 2014;192:808–13.
3. Chapple C, Andrich D, Atala A, Barbagli G, Cavalcanti A, Kulkarni S, et al. SIU/ICUD consultation on urethral strictures: The management of anterior urethral stricture disease using substitution urethroplasty. Urology. 2014;83:S31–47.
4. Fossati N, Barbagli G, Larcher A, Dell'Oglio P, Sansalone S, Lughezzani G, et al. The surgical learning curve for one-stage anterior urethroplasty: a prospective single-surgeon study. Eur Urol. 2016;69:686–90.
5. Cukierman E, Pankov R, Stevens DR, Yamada KM. Taking cell-matrix adhesions to the third dimension. Science. 2001;294:1708–12.
6. Debnath J, Mills KR, Collins NL, Reginato MJ, Muthuswamy SK, Brugge JS. The role of apoptosis in creating and maintaining luminal space within normal and oncogene-expressing mammary acini. Cell. 2002;111:29–40.
7. Farhat WA, Yeger H. Does mechanical stimulation have any role in urinary bladder tissue engineering? World J Urol. 2008;26:301–5.
8. Beiko DT, Knudsen BE, Watterson JD, Cadieux PA, Reid G, Denstedt JD. Urinary tract biomaterials. J Urol. 2004;171:2438–44.
9. Lin HK, Madihally SV, Palmer B, Frimberger D, Fung KM, Kropp BP. Biomatrices for bladder reconstruction. Adv drug Deliv Rev. 2015;82-83:47–63.
10. Song L, Murphy SV, Yang B, Xu Y, Zhang Y, Atala A. Bladder acellular matrix and its application in bladder augmentation. Tissue Eng Part B Rev. 2014;20:163–72.
11. Hu MS, Maan ZN, Wu JC, Rennert RC, Hong WX, Lai TS, et al. Tissue engineering and regenerative repair in wound healing. Ann Biomed Eng. 2014;42:1494–507.
12. Cen L, Liu W, Cui L, Zhang W, Cao Y. Collagen tissue engineering: development of novel biomaterials and applications. Pediatr Res. 2008;63:492–6.
13. Chattopadhyay S, Raines RT. Review collagen-based biomaterials for wound healing. Biopolymers. 2014;101:821–33.
14. Jia W, Tang H, Wu J, Hou X, Chen B, Chen W, et al. Urethral tissue regeneration using collagen scaffold modified with collagen binding VEGF in a beagle model. Biomaterials. 2015;69:45–55.
15. Rohman G, Pettit JJ, Isaure F, Cameron NR, Southgate J. Influence of the physical properties of two-dimensional polyester substrates on the growth of normal human urothelial and urinary smooth muscle cells in vitro. Biomaterials. 2007;28:2264–74.
16. Cui Y, Tan M, Zhu A, Guo M. Non-covalent interaction cooperatively induced stretchy, tough and stimuli-responsive polyurethane-urea supramolecular (PUUS) hydrogels. J Mater Chem B. 2015;3:2834–41.
17. El-Sherbiny IM, Yacoub MH. Hydrogel scaffolds for tissue engineering: progress and challenges. Glob Cardiol Sci Pr. 2013;2013:316–42.
18. Stier S, Rebers L, Schönhaar V, Hoch E, Borchers K. Advanced formulation of methacryl- and acetyl-modified biomolecules to achieve independent control of swelling and stiffness in printable hydrogels. J Mater Sci. 2019;30:35.
19. Jun I, Han H-S, Edwards R, Jeon H. Electrospun fibrous scaffolds for tissue engineering: viewpoints on architecture and fabrication. Int J Mol Sci. 2018;19:745.
20. Guo T, Yang X, Deng J, Zhu L, Wang B, Hao S. Keratin nanoparticles-coating electrospun PVA nanofibers for potential neural tissue applications. J Mater Sci. 2018;30:9.
21. Lv X, Guo Q, Han F, Chen C, Ling C, Chen W, et al. Electrospun poly(l-lactide)/poly(ethylene glycol) scaffolds seeded with human amniotic mesenchymal stem cells for urethral epithelium repair. Int J Mol Sci. 2016;17:1262.
22. Jia L, Han F, Wang H, Zhu C, Guo Q, Li J, et al. Polydopamine-assisted surface modification for orthopaedic implants. J Orthop Translation. 2019;17:82–95.
23. Yang B-Y, Deng G-Y, Zhao R-Z, Dai C-Y, Jiang C-Y, Wang X-J, et al. Porous $Se@SiO_2$ nanosphere-coated catheter accelerates prostatic urethra wound healing by modulating macrophage polarization through reactive oxygen species-NF-κB pathway inhibition. Acta Biomaterialia. 2019;88:392–405.
24. Shinchi M, Kushibiki T, Mayumi Y, Ito K, Asano T, Ishihara M, et al. Insulin-like growth factor 1 sustained-release collagen on urethral catheter prevents stricture after urethral injury in a rabbit model. Int J Urol. 2019;26:572–7.
25. Mathur R, Aggarwal G, Satsangi B. A retrospective analysis of delayed complications of urethroplasty at a tertiary care centre. Updates Surg. 2011;63:185–90.
26. O'Brien FJ. Biomaterials and scaffolds for tissue engineering. Mater Today. 2011;14:88–95.
27. Zhang K, Fu Q, Yoo J, Chen X, Chandra P, Mo X, Zhao W. 3D bioprinting of urethra with PCL/PLCL blend and dual autologous cells in fibrin hydrogel: an in vitro evaluation of biomimetic mechanical property and cell growth environment. Acta Biomaterialia. 2017;50:154–64.
28. Kotch FW, Raines RT. Self-assembly of synthetic collagen triple helices. Proc Natl Acad Sci USA. 2006;103:3028–33.
29. Shoulders MD, Raines RT. Collagen structure and stability. Annu Rev Biochem. 2009;78:929–58.
30. Adamowicz J, Juszczak K, Bajek A, Tworkiewicz J, Nowacki M, Marszalek A, et al. Morphological and urodynamic evaluation of urinary bladder wall regeneration: muscles guarantee contraction but not proper function - a rat model research study. Transplant Proc. 2012;44:1429–34.
31. O'Brien CM, Holmes B, Faucett S, Zhang LG. Three-dimensional printing of nanomaterial scaffolds for complex tissue regeneration. Tissue Eng Part B Rev. 2015;21:103–14.
32. Mousa NA, Abou-Taleb HA, Orabi H. Stem cell applications for pathologies of the urinary bladder. World J Stem Cells. 2015;7:815–22.
33. Jiang Y, Jahagirdar BN, Reinhardt RL, Schwartz RE, Keene CD, Ortiz-Gonzalez XR, et al. Pluripotency of mesenchymal stem cells derived from adult marrow. Nature. 2002;418:41–9.
34. Shakhssalim N, Soleimani M, Dehghan MM, Rasouli J, Taghizadeh-Jahed M, Torbati PM, et al. Bladder smooth muscle cells on electrospun poly(epsilon-caprolactone)/poly(l-lactic acid) scaffold promote bladder regeneration in a canine model. Mater Sci Eng C Mater Biol Appl. 2017;75:877–84.
35. Zakrzewski JL, van den Brink MR, Hubbell JA. Overcoming immunological barriers in regenerative medicine. Nat Biotechnol. 2014;32:786–94.
36. Zhang H, Jia X, Han F, Zhao J, Zhao Y, Fan Y, et al. Dual-delivery of VEGF and PDGF by double-layered electrospun membranes for blood vessel regeneration. Biomaterials. 2013;34:2202–12.
37. Drewa T, Adamowicz J, Sharma A. Tissue engineering for the oncologic urinary bladder. Nat Rev Urol. 2012;9:561–72.
38. Subramaniam R, Hinley J, Stahlschmidt J, Southgate J. Tissue engineering potential of urothelial cells from diseased bladders. J Urol. 2011;186:2014–20.